Journal of Colloid and Interface Science 516 (2018) 284–294

Contents lists available at ScienceDirect

Journal of Colloid and Interface Science

journal homepage: www.elsevier.com/locate/jcis

Regular Article

# Model lipid bilayers mimic non-specific interactions of gold nanoparticles with macrophage plasma membranes

Costanza Montis [a,*], Viola Generini [a], Giulia Boccalini [b], Paolo Bergese [c], Daniele Bani [b], Debora Berti [a]

[a] Department of Chemistry and CSGI, University of Florence, Via della Lastruccia 3, 50019 Sesto Fiorentino, Florence, Italy
[b] Department of Experimental and Clinical Medicine, University of Florence, Viale Pieraccini 6, 50139 Florence, Italy
[c] Department of Molecular and Translational Medicine, CSGI and INSTM, University of Brescia, 25123 Brescia, Brescia, Italy

## GRAPHICAL ABSTRACT

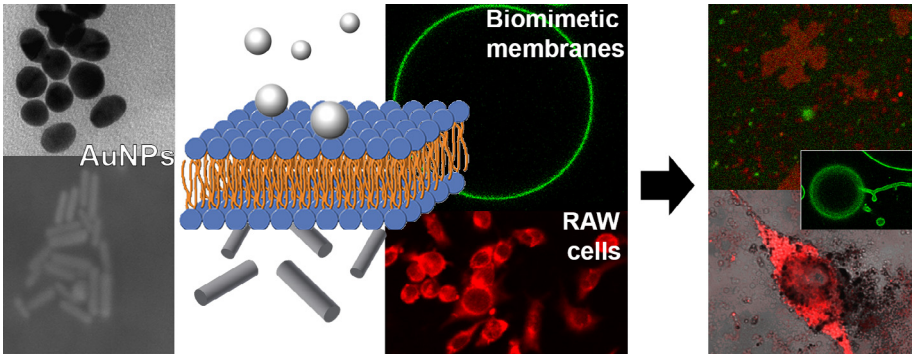


## ARTICLE INFO

*Article history:*
Received 6 December 2017
Revised 17 January 2018
Accepted 18 January 2018

*Keywords:*
Gold nanoparticles
Gold nanorods
Biomimetic membranes
Supported lipid bilayers
Giant unilamellar vesicles
Nanomedicine

## ABSTRACT

Understanding the interaction between nanomaterials and biological interfaces is a key unmet goal that still hampers clinical translation of nanomedicine. Here we investigate and compare non-specific interaction of gold nanoparticles (AuNPs) with synthetic lipid and wild type macrophage membranes. A comprehensive data set was generated by systematically varying the structural and physicochemical properties of the AuNPs (size, shape, charge, surface functionalization) and of the synthetic membranes (composition, fluidity, bending properties and surface charge), which allowed to unveil the matching conditions for the interaction of the AuNPs with macrophage plasma membranes *in vitro*. This effort directly proved for the first time that synthetic bilayers can be set to mimic and predict with high fidelity key aspects of nanoparticle interaction with macrophage eukaryotic plasma membranes. It then allowed to model the experimental observations according to classical interface thermodynamics and in turn determine the paramount role played by non-specific contributions, primarily electrostatic, Van der Waals and bending energy, in driving nanoparticle-plasma membrane interactions.



## 1. Introduction

Despite the abundance of fundamental and applied studies related to the *in vitro* therapeutic effects of inorganic nanoparticles (NPs), understanding the interaction of synthetic nanostructured matter with biological interfaces, and in particular cell membranes, is still an open challenge towards an effective clinical translation of nanotechnology- and nanotoxicology- related issues [1–7]. NPs injected in biological fluids are rapidly coated by a shell of biomolecules (often referred as corona) that, in subtle combination with the size and shape of the particles, (re)define the NP biological

* Corresponding author.
*E-mail address:* montis@csgi.unifi.it (C. Montis).

https://doi.org/10.1016/j.jcis.2018.01.064
0021-9797/

identity, including their interaction with cells and internalization pathways [8,9]. The first step of NP entry into cells is determined by their interaction with the cell membrane, which can lead to four main endocytosis mechanisms for mammalian cells, including phagocytosis, pinocytosis, caveolae endocytosis and clathrin mediated endocytosis [4,10]. This first step is often "non-specifically" driven by the high binding affinity of the NPs for the lipid membrane, which originates from the NPs excess surface energy. The biomembrane activity of inorganic or polymeric NPs, *i.e.* their tendency to structurally modify and/or permeate natural membranes, has been addressed in several studies on model synthetic membrane structures, as Giant Unilamellar Vesicles (GUVs) and Supported Lipid Bilayers (SLB) [11–13]. These reports suggest that several effects on membrane morphology, permeability and fluidity, such as formation of NP clusters onto the lipid bilayer or of lipid-raft-like domains, are driven by this first contact, and that they can be conveniently treated as a multiscale phenomenon to better capture the effect of the protein corona [14]. However, to date, a rational correlation between the findings on synthetic and real cell membranes is still lacking. We report here a first attempt in this direction. A library of gold nanoparticles (AuNPs), systematically covering sizes, charge, shape and coatings, with respect to nanomedicine applications, was prepared and tested in parallel on zwitterionic and anionic synthetic bilayers and eukaryotic immune system macrophage cells. The membrane activity of these NPs was investigated for free-standing (GUVs) and solid supported (SLBs) lipid bilayers of the same composition, with the twofold purpose to highlight the effect of membrane fluidity and to compare the insights from surface-based and solution techniques. Both GUVs and SLBs can be described as planar membranes [15], but the presence of a solid support in the latter case dramatically increases the energy necessary to bend the bilayer with respect to a GUV with the same composition. Macrophage cells were selected as they are involved in the immune system responses and reaction to external agents, and therefore they are highly relevant in the study of exogenous NP phagocytosis and toxicity [16]. NP-membrane interactions were monitored with Transmission Electron Microscopy (TEM) and Confocal Laser Scanning Microscopy (CLSM) and interpreted within the framework of the DLVO theory, which allowed us to provide a proof-of concept of the fidelity of solid-supported and free-standing synthetic bilayers as mimics of cell plasma membranes, with respect to unspecific interactions with inorganic NPs.

## 2. Materials and methods

### 2.1. Chemicals

Gold(III) chloride trihydrate (≥99.9%), Sodium citrate dihydrate (≥99.9%), poly(ethylene glycol) methyl ether thiol, (11-Mercaptoundecyl)-N,N,N-trimethylammonium bromide (≥90%), 11-mercaptoundecanoic acid (98%), Hexadecyltrimethylammonium bromide (≥99%), octanethiol (≥98.5%), ascorbic acid (≥98%), $AgNO_3$ (≥99%), toluene (99.8%), MeOH (99.8%), EtOH (≥99.8%), $CHCl_3$ (≥99%), $CH_2Cl_2$ (≥99.8%), THF (≥99.9%), boric acid (≥99.5%), NaCl (≥99.5%), Calcium chloride hydrate (99.999%), Tetraoctylammonium bromide (98%), glucose (≥99.5%), sucrose (≥99.5%), borax (≥99%), $NaBH_4$ (≥98%) were provided by Sigma-Aldrich (St. Louis, MO). The same for Fetal Bovine Serum (FBS) and (3-(4,5-dimethylthiazol-2-yl)-2,5-diphenyltetrazolium bromide (MTT) for cells treatment. CellMask™ Orange Plasma membrane stain and β-Bodipy 2-(4,4-diuoro-5,7-dimethyl-4-bora-3a,4adiaza- sindacene- 3-pentanoyl)-1 hexadecanoyl-sn-glycero-3-phosphocholine) were purchased from Invitrogen Life Technologies (Heidelberg, Germany), while $DiIC_{20}$ (1,1′-dieicosanyl-3,3,3′,3′-tetramethylindocarbocyanine perchlorate) was purchased from Molecular Targeting Technologies (Westchester, PA). 1-palmitoyl-2-oleoyl-sn-glycero-3-phosphocholine (POPC, >99%) and 1-palmitoyl-2-oleoyl-*sn*-glycero-3-phospho-(1′-*rac*-glycerol) (sodium salt) (POPG, >99%) are from Avanti Lipids (Alabaster, AL). All chemicals were used as received. Milli-Q grade water was used in all preparations. The synthetic procedures for AuNPs are reported in the Supplementary Materials and Methods (SI).

### 2.2. GUVs preparation

Giant Unilamellar Vesicles were prepared through electroformation [17–19]. Briefly, a POPC or POPG:POPC 1:1 0.5 mg/ml stock solution in $CHCl_3$ was prepared and 0.1% with respect to the total lipid amount of the fluorescent dye (β-Bodipy) was added. 10 μl of the stock solution were deposited on each of two ITO-coated glass slides, on the conductive side. Chloroform was dried under vacuum for two hours and a dry lipid film on each sheet was obtained. The electroformation chamber was prepared sandwiching the sheets with an O-ring separating the lipid films. The chamber was filled with an aqueous solution of sucrose 15 mM, and the electrical contact between the sheets was provided by putting on each sheet a copper tape connected to a pulse generator, set at a sinusoidal alternating voltage of 10 Hz frequency and 2 Vpp amplitude for two hours. GUVs were employed within 24 h after preparation.

### 2.3. SLBs preparation

For Small Unilamellar Vesicles preparation the proper amount of POPC or POPG and POPC was dissolved in chloroform/methanol 6:1 (v/v). A lipid film was obtained by evaporating the solvent under a stream of nitrogen and overnight vacuum drying. The film was then swollen and suspended in warm (50 °C) NaCl 100 mM solution by vigorous vortex mixing. To prepare Unilamellar vesicles (ULV) with narrow distribution, the dispersion was then tip-sonicated for 30 min. SLB were prepared by adding 10 mM $CaCl_2$ to the vesicles' dispersion and subsequently injecting the vesicles in a chamber containing a coverglass on the bottom. A stable SLB layered on the coverglass was obtained by rinsing the vesicles' dispersion with pure milliQ water, after incubation of the vesicles with the coverglass for twenty minutes at r.t. To fluorescently label the SLB, a small amount of fluorescent probes (β-Bodipy and $DiIC_{20}$), *i.e.*, 0.1% mol:mol with respect to total lipid amount was added.

### 2.4. Cell culture

Mouse RAW 264.7 macrophages were obtained from the European Collection of Cell Cultures (ECACC, Salisbury, UK). Cells were maintained in Dulbecco's modified Eagle medium (DMEM) supplemented with 10% fetal bovine serum (Gibco Invitrogen, Milan, Italy), 100 U/ml penicillin-streptomycin, 1% l-glutamine 200 mM, (Sigma-Aldrich, Milan, Italy) and 4.5 g/l glucose, and grown in 5% $CO_2$ atmosphere at 37 °C.

### 2.5. Confocal Laser Scanning microscopy (CLSM)

CLSM experiments were carried out with a laser scanning confocal microscope Leica TCS SP2 (Leica Microsystems GmbH, Wetzlar, Germany) equipped with a 63× water immersion objective. The 488 nm laser line was employed to detect β-Bodipy fluorescence (λexcitation 488 nm, λ emission 498 nm–530 nm); the 561 nm laser line was employed to detect $DiIC_{20}$ and Cell Mask dye inside the cells' membrane (λexcitation 561 nm, λ emission 571 nm–650 nm); the 633 nm laser line was employed to detect AuNP